Mine Water and the Environment (2020) 39:268–279
https://doi.org/10.1007/s10230-020-00683-w

TECHNICAL ARTICLE

Full-floor Grouting Reinforcement for Working Faces with Large Mining Heights and High Water Pressure: a Case Study in China

Shiqi Liu[1,2] · Yu Fei[1] · Yanchun Xu[1] · Lei Huang[1] · Wenyan Guo[1,3]

Received: 25 March 2019 / Accepted: 15 April 2020 / Published online: 23 April 2020

Abstract
Grouting reinforcement was used to safely and efficiently exploit the thick coal seam in the Jiaozuo coalfield. First, the water inrush possibility of the 11,050 working face was evaluated, using both the floor failure depth and the water bursting coefficient (T) methods. The estimated depth of the floor failure zone (h) ranged from 22 to 38 m, which is larger than the average distance between the floor-confined aquifer (L_8) and the no. 2 coal seam. Additionally, the water bursting coefficient of L_8(0.268) was much higher than the ultimate T_s(0.100). Thus, the evaluation showed that the L_8 confined limestone aquifer had a high water inrush possibility. Innovative grouting methods and supporting facilities, such as dispersed pulping, repeated pipe fixation, and three-stage flange structure, were proposed to address the threat. Finally, both drilling and geophysics (i.e. DC method) indicated that the grouting reinforcement had been effective.

Keywords Floor water inrush · DC electrical method

Introduction

The exploitation of coal resources in China is seriously threatened by water hazards, which have caused serious casualties and economic losses. It is estimated that more than 50% of China's major coal mines are threatened by water hazards (Ren 2015). Water hazards are mainly caused by poorly sealed boreholes and mining-induced fractures (Luo and Peng 2005; Zhang et al. 2004; Zhang et al. 2015; Zhao et al. 2015). Confined aquifers are the most common water inrush sources throughout China. Some investigations (Wu et al. 2004; Zhang 2005; Wang and Park 2003) have shown that using short-wall, room and pillar, or strip pillar mining methods can reduce the risk of water inrush. However, over 90% of China's underground coal mines use longwall mining. Thus, it is imperative to study the mechanisms of water inrush, especially those induced by confined aquifers, and preventive measures.

Methods used to evaluate water inrush possibilities include empirical formulas, numerical simulations, and theoretical analyses. Many statistical formulas were obtained to predict the depth of the destructive floor and to conduct a regression analysis (Xu and Yang 2013). In addition, crack connection and propagation models (Chen et al. 2016) were used to obtain the hydraulic conductivity of deep rock formations to evaluate the risk of floor water inrush. The hydraulic conductivity can be used to characterize the water inrush coefficient, and thus, the direct current (DC) electric method for assessing the risk of water inrush was proposed (Lu and Wang 2015; Meng et al. 2012). It is understood that floor water inrush always occurs later than coal extraction, and this phenomenon is a gradual, time-related process. Some models are good predictors of water inrush zones, such as Fisher's discriminant model (Chen et al. 2016).

There are two main ideas to prevent water inrush: one is to dewater the aquifer, and the other is to fill the cracks in the rock. Specific water inrush preventive measures include water pumping (pressure release) (Meng et al. 2018), ground treatment, underground grouting reinforcement (Hu et al. 2019), and curtain grouting (Zhou et al. 2017). Extracting the water from the aquifer and reducing the water pressure

✉ Yu Fei
13573256450@163.com

[1] School of Energy and Mining, China University of Mining and Technology, Beijing 100083, People's Republic of China

[2] Hebei State Key Laboratory of Mine Disaster Prevention, North China Institute of Science and Technology, Beijing 101601, People's Republic of China

[3] National Key Lab of Coal Resources High Efficient Mining and Clean Utilization, China Coal Research Institute, Beijing 100013, People's Republic of China

is the fundamental way to resolve the problem, but this can be difficult and expensive. Moreover, the large decrease in the groundwater level can consolidate and compress the rock and soil, thereby increasing the possibility of damage to the surface and the environment.

Grouting can replace the water in cracks, while also reinforcing the strength of rock formation. Moreover, this method has less impact on the water environment, especially near the surface. There are many factors that affect mine floor stability, including ground stress, formation pressure, mining scale, geological structure, and floor water pressure. The grouting program should be adjusted for different conditions. The main method to reduce the risk of floor water inrush from coal mines is grouting, and many mines have used this approach. Li et al. (2017) put forward a grouting solution based on statistical analysis of borehole deviation, at a site where the aquifer was close to the coal seam. Two main factors (Sui et al. 2015) that affect the effectiveness of grouting are the initial water flow speed and the aperture width. The grouting reinforcement techniques of these examples were mostly used at sites with a small aquifer water pressure and cannot be used when the aquifer pressure is too large and close to the coal seam. It is important to study and improve grouting technology, especially grouting parameters.

The Zhaogu no. 2 coal mine is located in the Jiaozuo coalfield, where have been more than 500 water inrushes; the maximum water inrush amount reached 19,200 m^3/h, which resulted in serious casualties and heavy property losses. Thus, there was a high water inrush risk to the 11,050 working face, and so a full-floor grouting project was implemented before mining. However, there are very few sites where this approach has been successfully used with such extremely high floor water pressure.

Geology and Hydrology of the Study Area

Overview of the 11,050 Working Face

The Zhaogu no. 2 coal mine is located in the eastern Jiaozuo mining area, which is known for its abundant water and the high hydraulic pressure in the limestone layers close to its 2–1 coal seam. The Jiaozuo coalfield is located in northwest Henan Province, China (Fig. 1). The Zhaogu no. 2 coal mine is a modern mine with a production capacity of 1.8 million metric tons per year. The 11,050 working face is ≈ 2131.9 m wide along the dip and 180 m long along the strike. The average thickness of the 2–1 coal seam is 6.32 m, the average dip angle is 5.5°, and the buried depth is 682 m. Full-seam, fully mechanized, and retreating mining methods are used at the working face.

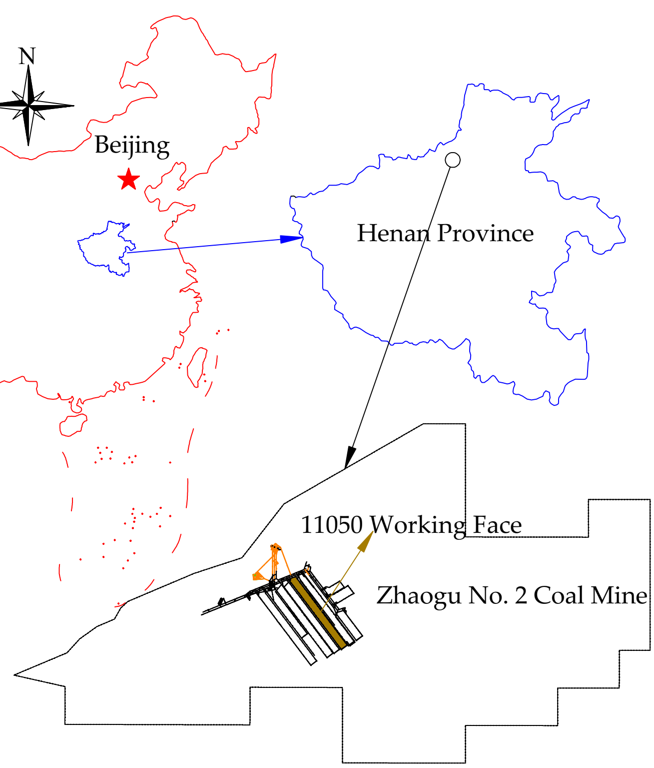

Fig. 1 Location of the study area

Structure of the 2–1 Coal Seam Floor

There are 3 main limestone aquifers in the 2–1 coal seam floor, i.e. the L_8 limestone aquifer in the upper part of the Taiyuan group, the L_2 limestone aquifer in the lower part of the Taiyuan group, and the Ordovician limestone aquifer (Fig. 2). Most of the rest of the floor strata are mudstone layers, with some thin sandstone layers. Additionally, the mudstone layers can be divided into 3 aquiclude groups, i.e. the immediate floor sand-mudstone aquiclude, the Taiyuan group mudstone aquiclude and the Benxi group aluminum mudstone aquiclude.

The L_8 Limestone Aquifer

According to data from 30 boreholes within the 11,050 working face, the L_8 limestone aquifer is the most developed; it is 6.77–14.78 m thick (8.3 m on average), and is abundantly fractured. L_8 is a medium water-rich aquifer with a static water level of + 80.49 to + 84.97 m. Its unit water discharge is 0.0005–0.059 L/(s m), and its permeability coefficient is 0.0036–0.648 m/d. The distance between the L_8 aquifer and the 2–1 coal seam is 19.10–29.22 m (26.5 m on average). Its water pressure is ≈ 7.09 MPa. Obviously, L_8 is the most threatening floor aquifer to the 11,050 working face.

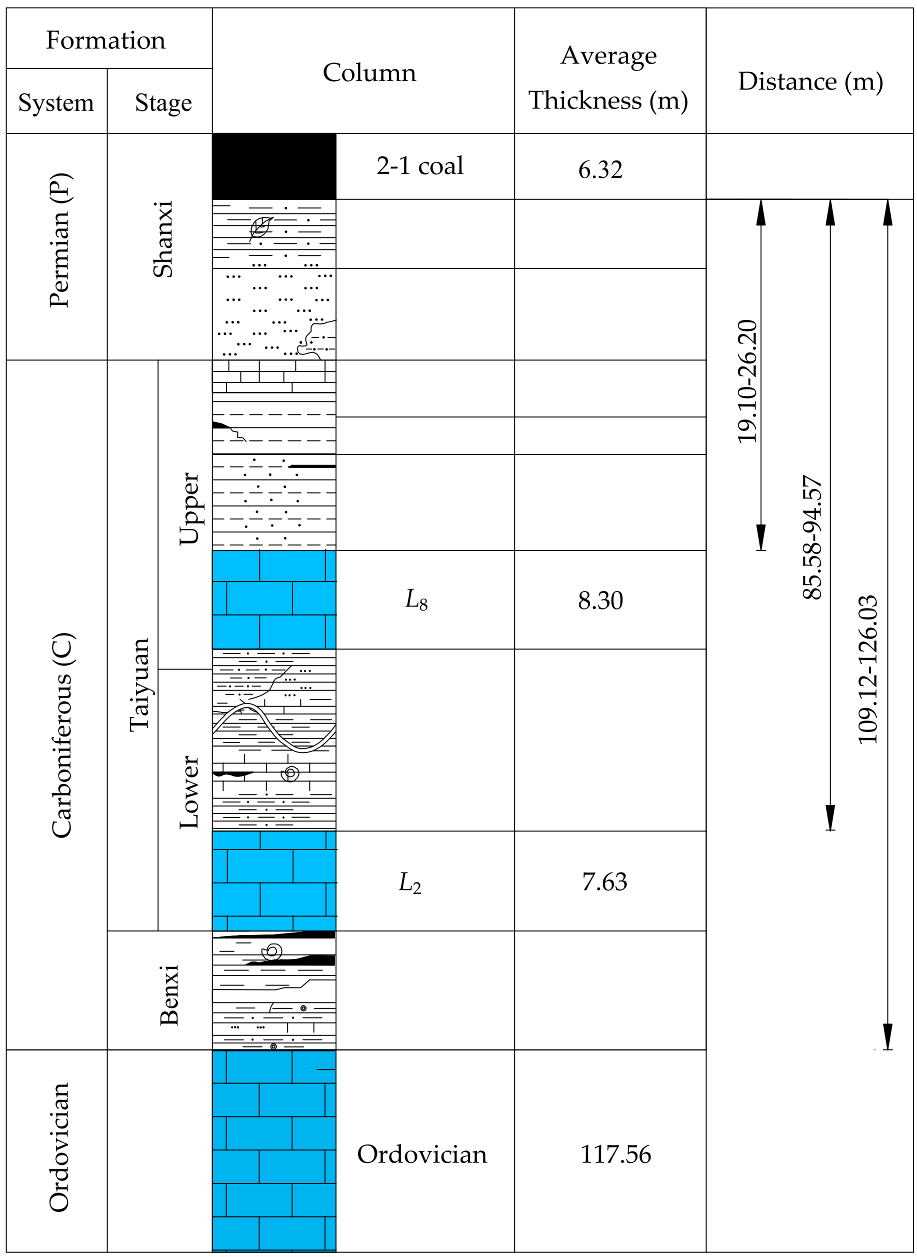

Fig. 2 Composite column of the 11,050 working face floor

The L_2 Benxi Group Limestone Aquifer

The L_2 is 10.01–14.68 m thick, with an average of 12 m. Additionally, the thickness increases gradually from west to east within the mine area. The distance between L_2 and the 2–1 coal seam is 85.58–94.57 m (88.88 m on average), and it is ≈ 20 m from the top of the Ordovician limestone layers. The static water level of L_2, which belongs to a strong water-rich aquifer, is now + 33 m to + 82 m. Its average unit discharge is 1.090 L/(s·m), and its permeability coefficient is 9.87 m/d. The water pressure of the L_2 limestone aquifer is 7.63 MPa. Karst cracks are well developed in L_2, and studies show that there is an obvious hydraulic connection between L_2 and the strong water-rich Ordovician limestone aquifer. Thus, L_2 is a key aquifer for the prevention of water inrush.

The Ordovician Limestone Aquifer

This aquifer is mainly composed of limestone and argillaceous limestone layers in the Majiagou group. The Ordovician aquifer is extensive, with a thickness ranging up to 67.30 m in this hydrogeological area according to exploratory data from 9 boreholes. The buried depth of the Ordovician aquifer is 725.86–991.50 m, and it is 109.12–126.03 m (117.56 m on average) away under the 2–1 coal seam. The Ordovician aquifer has a relatively steady water level of + 79- + 85 m within the entire mine field, and its average water pressure is 9.01 MPa.

The Immediate Floor Sand-Mudstone Aquiclude

This section refers to the layers that are located between the 2–1 coal seam and L_8. The lithology of this aquiclude includes aluminum mudstone, sandy mudstone, and sandstone. It is 9.1–17.27 m thick with an average of 12.84 m. This section has a stationary distribution with good water-resistant properties, but the stability of its water-resisting properties under the influence of mining deserves further study.

The Taiyuan Group Mudstone Aquiclude

This section is located below L_8 and above L_2. This section is 35.22–48.90 m thick, with an average of 43 m. This aquiclude is mainly composed of mudstone layers, with some thin sandstone and limestone layers.

The Benxi Group Aluminum Mudstone Aquiclude

This section is above the Ordovician aquifer and under L_2 and is 4.5–12.63 m thick. The lithology is mainly aluminum mudstone. It is well developed within the study area but is too thin to be significant.

Physical and Mechanical Properties of Floor Rocks

Hard and brittle rocks are prone to cracking under the stress caused by mining, but the cracks are not easily enlarged by high water pressure. In contrast, soft rocks will not easily crack, but plastic deformation will occur. There are even initial fissures and damage cracks; the soft rock layers have poor permeability because of the clay clasts between their structural surfaces. However, the cracks are easily enlarged by high water pressure. If the aquiclude is composed of hard and soft rock layers, the advantages of both are combined and its water resistance is improved. According to the stress intensity factor, the cracks in hard rock formations tend to expand into soft rock formations, but the cracks in soft rock formations do not easily expand into hard rock formations. Therefore, the most favourable combination of lithology is soft rock formations on the top and bottom with a middle section that is interbedded with soft and hard rock formations.

As seen from Fig. 2, the lithology of the 2–1 coal seam floor from top to bottom in the Zhaogu no. 2 coal mine is sandy mudstone, fine sandstone, sandy mudstone, limestone, medium sandstone, sandy mudstone, mudstone, and limestone. This lithology combination basically coincides with the above rule and provides favourable conditions for preventing water inrush from the floor aquifers.

According to the drilling statistics, the rock quality designation (RQD) of the mudstones is 44.3–66.8%, and that of the sandy mudstones and sandstones is 31.9–100%. Therefore, the integrity of the floor rock strata in the 11,050 working face is good. The lithological rock mechanical indicators of the coal and floor rock mass are listed in Table 1.

From Table 1, we can see that the mechanical strength of the floor rock is obviously different under dry and saturated conditions. The strength of the mudstone and sandy mudstone obviously decreases after absorbing water, which is unfavorable for water inrush prevention of a floor broken by mining activities.

Assessment of Floor Water Inrush

Possibility of Water Inrush Based on the Floor Failure Depth

Experience Formula Method

During coal seam mining, the original stress state is changed, resulting in cracks in the floor rock and groundwater bursting through the cracks. Therefore, it is important to calculate the depth of the floor failure zone. The study shows that the main factors affecting the depth of the failure zone include the buried depth H, coal seam angle α,

Table 1 Rock mechanics index of the 11,050 working face floor

Lithology	Compressive strength (MPa)		Tensile strength (MPa)	Softening coefficient	Internal friction angle (°)	Cohesion (MPa)
	Dry	Saturated				
Coal	8.32	/	0.13	/	28°01′	1.05
Medium Sandstone	36.0–44.0	16.4–20.8	2.0–2.7	0.45	35°10′	7.2
Fine Sandstone	35.6–68.4	23.2–48.0	1.2–2.3	0.59–0.65	35º45´–36º47´	5.5–8.1
Siltstone	40.8–84.0	24.8–43.6	1.8–3.3	0.52–0.66	30º45´–40º23´	7.5–11.0
Mudstone	23.3–29.2	5.2–11.2	0.8–1.0	0.31	32º36´	5.0
Sandy Mudstone	15.2–31.2	4.4–14.0	0.3–1.5	0.30–0.40	32º06´–36º07´	4.1–5.3

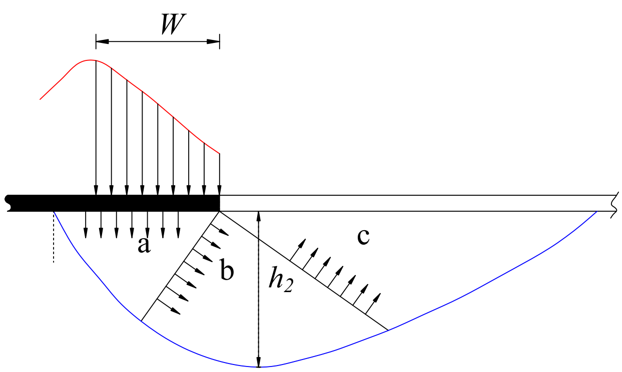

Fig. 3 Failure diagram of coal seam floor with pressure: a-active failure zone (Rankine zone). b-transitional zone. c-passive failure zone (passive Rankine zone)

working face inclined length L, mining height M, floor rock destruction intensity, and structure. At present, the methods for calculating the depth of the failure zone mainly include the statistical equation, the fracture mechanics equation, and the plastic mechanics method. The statistical equation is obtained from the measured data collected from various mines and is widely used in China (State Bureau of Coal Industry 2000):

$$h_1 = 0.0085H + 0.1665\alpha + 0.1079L - 4.3579 \tag{1}$$

where h_1 is the floor failure depth, H is the buried depth of the coal seam, L is the length of the working face, and α is the angle of the coal seam. Taking 682 m for H, 5.5° for α, and 180 m for L, the floor failure depth of the 11,050 working face was estimated as: $h_1 = 21.78$ m.

Plastic Mechanics Method

Figure 3 shows the floor failure zone of the longwall working face during mining. W and h_2 are the plastic zone width and the maximum floor failure depth (W), respectively. According to the theory of plastic mechanics, W and h_2 are derived as follows (State Bureau of Coal Industry 2000):

Table 2 Estimated results of the floor failure depth

Calculation	Empirical Formula	Plasticity Mechanics
Depth of failure zone (m)	21.78	37.03

$$W = \frac{m}{2K\tan\varphi}\ln\frac{n\gamma H + C_m\cot\varphi}{KC_m\cot\varphi} \tag{2}$$

$$h_2 = \frac{W\cos\varphi_0}{2\cos\left(\frac{\pi}{4} + \frac{\varphi_0}{2}\right)}e^{\left(\frac{\pi}{4}+\frac{\varphi_0}{2}\right)\tan\varphi_0} \tag{3}$$

where n is the maximum stress concentration factor, m is the mining height, H is the buried depth of the coal seam, γ is the rock mass density, C_m is the cohesion of coal, φ is the internal friction angle of coal, φ_0 is the average internal friction angle of floor rock mass, and K is short for $(1+\sin\varphi)/(1-\sin\varphi)$.

According to Table 1, taking φ as 28°, n as 1.6, C_m as 1.05 MPa, m as 6.5 m, γ as 25.48 kN/m^3, and H as 682 m, the plastic zone width can be calculated using Eq. (2): $W = 18.89$. Therefore, using Eq. 3, and $\varphi_0 = 37°$, we can obtain the maximum floor failure depth: $h_2 = 37.03$ m.

Table 2 shows the results of the floor failure depth of the 11,050 working face using different calculation equations. The average distance between floor L_8 and the 2–1 coal seam is 25.5 m, while the depth of the failure zone is expected to range from 21.78 m to 37.03 m. The floor failure zone may extend to the L_8 aquifer, so there was a significant possibility that the water from L_8 could rush into the 11,050 working face. The distance between L_2 and the 2–1 coal seam is much larger than the maximum floor failure depth of the 11,050 working face, so a direct water inrush from L_2 is less likely. However, L_8 may somehow connect with L_2 through faults or other fracture structures. Thus, L_8 is the key stratum that determines whether a water inrush occurs.

Table 3 Critical water-bursting coefficient in some Chinese mine areas

Mining area	Fengfeng and Handan	Zibo	Jiaozuo	Jingxing
T (MPa·m^{-1})	0.066 ~ 0.076	0.060 ~ 0.140	0.060 ~ 0.100	0.060 ~ 0.150

Table 4 T values of the L_8, L_2, L_3, and Ordovician aquifers

Aquifer	P (MPa)	M (m)	h (m)	T (using Eq. 4) (MPa·m^{-1})	T (using Eq. 5) (MPa·m^{-1})
L_8	7.09	26.5	37.03	0.268	/
L_2	7.63	88.88	37.03	0.086	0.147
Ordovician	9.01	117.56	37.03	0.077	0.112

Table 5 Detection data of some test holes

Hole no.	Water inflow (m^3/h)	Water pressure (MPa)	Aquifer
T01-01	66.30	7.60	L_2
T01-02	11.82	6.99	L_8
T02-01	32.06	7.03	L_8
T02-02	14.25	6.98	L_8
T03-01	27.89	7.01	L_8
T04-01	33.30	7.01	L_8
T05-01	12.87	6.98	L_8
T05-02	76.28	7.62	L_2
T06-03	49.44	7.61	L_2

Possibility of Water Inrush Based on the Water-bursting Coefficient

The water-bursting coefficient (T) is defined by the water pressure bearing capacity per unit thickness of the floor aquiclude, and is an important parameter in the floor water control. The equation of the water inrush coefficient is derived as follows (State Bureau of Coal Industry 2000):

$$T = \frac{P}{M} \tag{4}$$

where P is the water pressure from the confined aquifer, and M is the thickness of the waterproof strata. Taking the floor failure depth into account, Eq. (4) can be changed as follows:

$$T = \frac{P}{M - h} \tag{5}$$

where h is the depth of the floor failure zone.

The critical water-bursting coefficient (T_s) is the maximum water pressure that can be sustained by the efficient thickness of the floor strata. If the calculated result of the water-bursting coefficient is less than the critical water-bursting coefficient ($T < T_s$), the floor is considered to be stable, and the possibility of water inrush is small. However, if $T \geq T_s$, the floor is unstable, and the possibility of water inrush increases. T_s is derived from water inrush records of many mines across China, and some of the values are shown in Table 3. It is important to remember that the T_s data in Table 3 were calculated by Eq. (4). In this paper, we take 0.060 as the initial T_s and 0.100 as the ultimate T_s. If T is larger than the ultimate T_s, measures must be taken.

The T values of the L_8, L_2, L_3 and the Ordovician aquifers were estimated using Eqs. (4) and (5) (Table 4). As expected, the floor failure depth is greater than the distance between L_8 and the 2–1 coal seam, so the T value of L_8 (0.268) is much higher than the ultimate T_s (0.100), which means that there is a high water inrush possibility from the L_8 aquifer. We can also see from Table 4 that the T values of the L_2 and Ordovician aquifers are 0.086 and 0.077, respectively, which means that the probability of water inrush from the L_2 or Ordovician aquifers is high, but not necessarily absolute. Through this analysis, we understand that L_8 is the key grouting target and that reinforcing L_8 will reduce the water inrush risk from L_2 and the Ordovician aquifer.

Possibility of Water Inrush Based on Drilling

During the gateway excavation, some holes were drilled to test the water quantity and water pressure of the floor-confined aquifers. Some of the results are shown in Table 5.

For the Zhaogu no. 2 coal mine, it was considered safe if the water flow of each detection hole was less than 10 m^3/h; otherwise, measures must be taken to address the water inrush risk. We can see in Table 5 that the water inflow of each detection hole was much higher than 10 m^3/h. Additionally, the largest water inflow of L_8 was approximately 33.30 m^3/h.

The above analysis shows that the risk of water inrush from the floor is high. The mining height leads to a large floor failure depth, and the resulting cracks are more likely to be connected to the aquifer. So, the full-floor needs to be grouted and reinforced to fill the cracks and reduce the aquifer water pressure; the only other safe alternative would be to reduce the mining height.

Grouting Reinforcement Technique

"Pore-fractured Lifting Type" Model

Based on the fracture fragmentation and connectivity of floor rock, "pore-fractured lifting type" model (Xu and Li 2014) divides a rock mass into four types (see Fig. 4): a complete water-tight rock mass (type I), a non-connected fractured rock mass (type II), a connected fractured rock mass (type III), and a broken rock mass (type IV).

The reservoir space of a type I rock mass is mainly matrix pores, so this type of rock mass can be regarded as homogeneous and waterproof, e.g. an intact shale layer. There may be some secondary cracks in a type II rock mass, but the cracks, which are mainly caused by tectonic movements, are unconnected. Therefore, a type II rock mass has a high water storage capacity but low permeability. In a type III rock mass, the cracks are both abundant and connected. Type III rock layers, most of which are natural strong aquifers, have a large water storage capacity and high permeability. Formed under the disturbance of large tectonic movements or mining activities, type IV rock masses are highly fractured. There are both main fracture zones and ancillary fracture zones for water flow in a type IV rock mass, so it is highly permeable.

Mining can increase the rock type in a rock mass; for example, type I, II or III rock masses can be changed into a type IV rock mass by mining. Grouting reinforcement can be used to improve the water-resistance of a rock mass, by filling the rock fracture with slurry. Thus, grouting can lower the rock type of a rock mass; for example, type II, III or IV rock masses can be changed into a type I rock mass by grouting.

For this project, the floor layers of the 2–1 coal seam were classified based on the drilling results. The rock masses in the L_8, L_2 and Ordovician strata were classified as type III. The immediate floor sand-mudstone was type I, but likely to be raised to type IV by mining. The mudstone rock masses in the Taiyuan and Benxi groups have good structural integration and are type I. Therefore, the grouting goals were to decrease the L_8 rock mass type and strengthen the physical and mechanical properties of the immediate floor sand-mudstones.

Project Design for Full-floor Grouting

Considering the previous analysis along with an economic feasibility analysis, L_8 was the key grouting object, and L_2 was the key prevention target. Therefore, the vertical height of the grouting was designed for the ceiling of the L_2 stratum, in which the water pressure was too high to control if the grouting boreholes contacted it. The distance between L_2 and the 2–1 coal seam was 85.6–104.6 m. The largest vertical distance of a borehole below the 2–1 coal seam was ≈ 85 m and the largest horizontal distance was 30 m from the working face gateways.

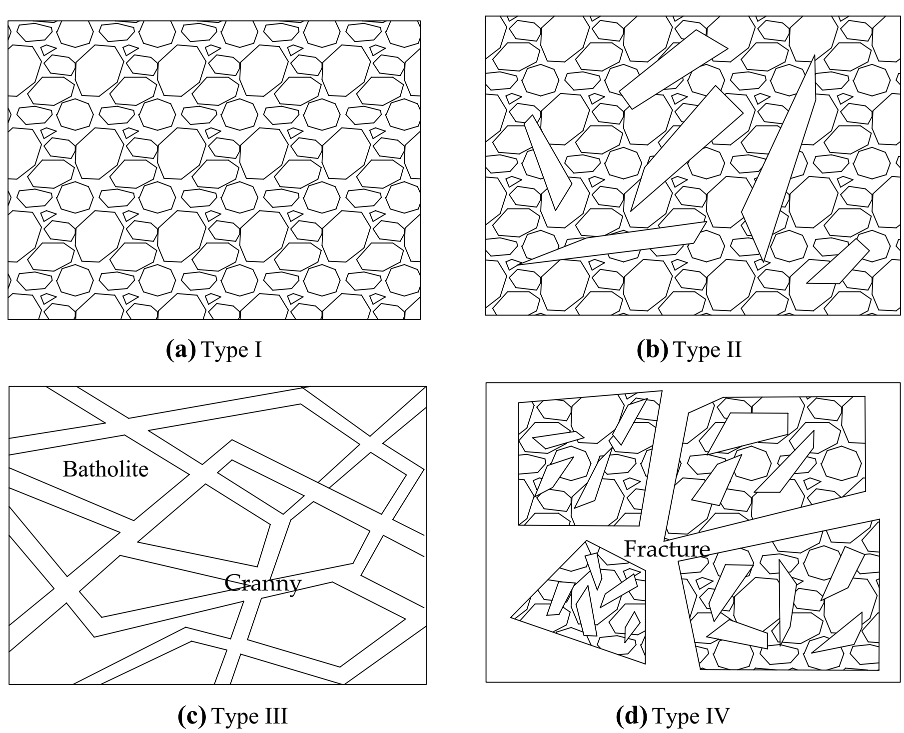

Fig. 4 Types of rock mass. **a** Type I. **b** Type II. **c** Type III. **d** Type IV

Grouting pressure is affected by many factors, such as hydrogeological conditions, hydrostatic pressure, aquifer permeability, and aquifer water flow rate. Based on experiences in many parts of China, such as Jiaozuo, Fengfeng and other mining areas, the grouting pressure in these areas was adjusted to be 2–3 times the hydrostatic pressure of the aquifer. The water pressure of the L_8 limestone aquifer was 7.09 MPa in the Zhaogu no. 2 coal mine. The designed grouting pressure was twice the pressure in L_8 that is, 14.18 MPa; therefore, the practical grouting pressure was set at 15 MPa.

Clay cement consists of 80% clay and 20% cement. The specific gravity of the clay slurry was 1.10–1.18, and the sand content was less than 5%. When the mud leakage exceeded 20% of the grouting amount, kelp, soybean, and sawdust were also used to fill large cracks.

According to the previous site test results, the average diffusion radius of grouting slurry was ≈ 20 m. To ensure adequate grouting reinforcement of the 11,050 working face, 42 drilling sites in total were arranged in both the head-entry and the tail-entry. The distance between the two sites was 100 m. Each site was 5 m long, 5 m wide, and 3.8 m high. Ten drilling holes, including eight injection holes and two test holes, were designed in each area. Figure 5 shows the drill hole arrangement for the first 500 m of the 11,050 working face. We can see that 12 drilling sites and 137 holes were constructed, and that the average length of each hole was ≈170 m.

Implementation of the Floor Grouting Reinforcement Project

To guarantee grouting quality under high water pressures, some new grouting methods were used, such as dispersed pulping, transport by thin pipe, and repeated pipe fixation. These terms are described below.

System of Grouting

To ensure the quality of the cement slurry and enhance the ratio elasticity of the cement and clay slurry, the dispersed pulping technique was used in the Zhaogu no. 2 coal mine. Different from the more widely used long-single-hole directional grouting, the dispersed pulping method requires a lot of short drilling holes. This ensures that the grout reaches the entire grouting area. This involved making the cement and clay slurries separately in high-speed vortex pulper (we used Xinyan Mining Mechanical Equipment Co.'s. model ZJ-400X), and then mixing them in varying proportions in accordance with the grouting requirements. There are many advantages to this technique, such as a smooth slurry, strong fluidity, no bubbles in the slurry, and a large diffusion range. The density of the slurry was controlled between 1.1 and 1.7 g/cm^3, and 8.8 tons of slurry could be produced per hour.

To prevent plugging and ensure continuous grouting operations, the inner diameter of the grouting pipes was changed from 120 to 60 mm. Thus, the running velocity of the slurry was accelerated, which reduced precipitation and plugging in the pipes. Both the grouting steel pipe and the steel-wire hose could withstand high pressures; for example, the compressive strength of the steel-wire hose was greater than 20 MPa. The grouting pipes were fixed on the opposite side of the roadway to avoid harming walking workers if leakage occurred.

A three-stage flange structure (see Fig. 6) connected each flange in a chain to enhance the compression and tensile strength and to prevent pipe cracking, deformation, and leakage under high water pressure conditions.

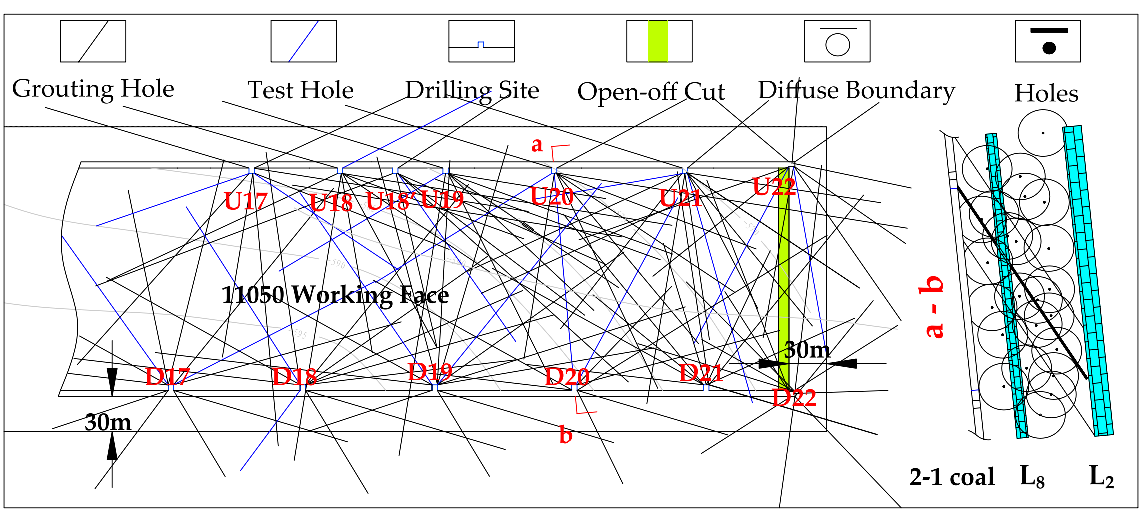

Fig. 5 Layout of grouting holes in the first 500 m of the 11,050 working face

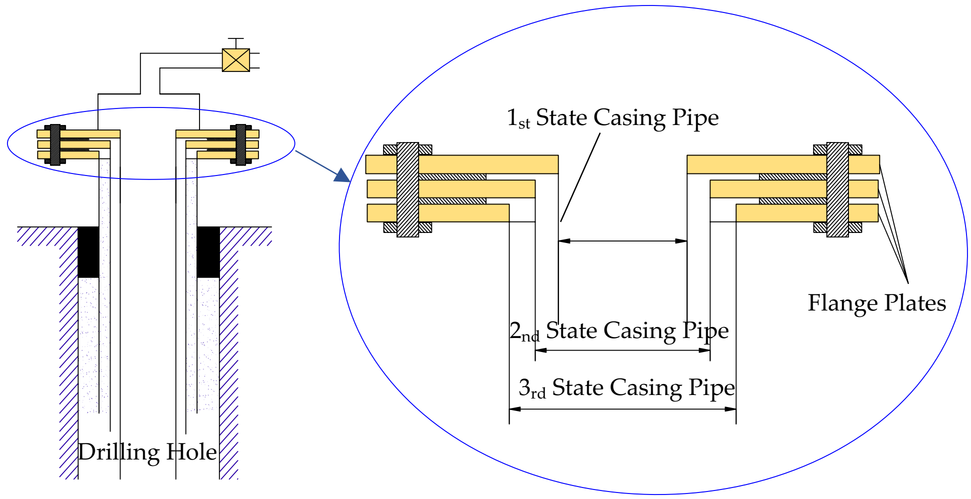

Fig. 6 The three-stage flange structure

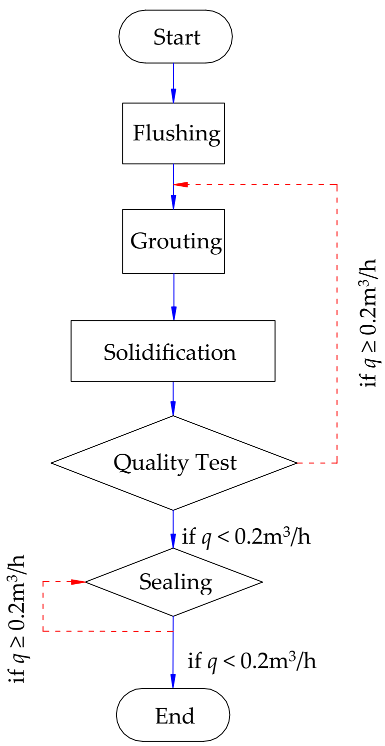

Fig. 7 Grouting process

Additionally, the repeated pipe fixing method was used; this means that fact that the pipes were affixed to the hole wall three times as much as usual, using sodium silicate or cement paste after each pipe was installed. Together, these two methods guaranteed that the pipes could sustain a grouting pressure of 15 MPa.

Process of Ultra-High Pressure Grouting

The grouting process of one grouting hole can be summarized as follows: hole flushing, grouting, solidification, hole sealing and examination (Fig. 7). The grouting effect can be evaluated by using the aquifer permeability coefficient K, which is calculated by the Dupuit formula,

$$K = 0.366Q\frac{lgR - lgr}{m \times s} \tag{6}$$

where Q is drilling water inflow;R is the radius of influence when pumping water; r is the drilling radius; m is aquifer thickness; and s is the water table reduction.

First, the finished grouting hole was flushed with fresh water before grouting to reduce the quantity of rock powder and fragments. Second, the main process of grouting was carried out. The slurry density was adjusted and stabilized at ≈ 1.30 g/cm^3 before grouting. Additionally, the standard of qualified grouting was that the injection pressure had to be stabilized at 15 MPa. Third, the injection valve was closed after grouting and the slurry was allowed to solidify for at least 30 h. Fourth, the grouting effectiveness was tested by drilling a hole to the bottom again. Based on site experience, the water inflow (q) had to be less than 0.2 m^3/h; otherwise, the grouting and subsequent operations were carried out again. After all of the grouting holes in one site were qualified, the test holes were constructed. The standard for this test hole was that water inflow had to be less than 10 m3/h. Finally, all of the grouting and test holes were sealed with a cement-silicate (CS) slurry. The sealing quality was good if the water inflow was less than 0.2 m^3/h from the hole after CS solidification. Otherwise, the holes had to be sealed again until they met this requirement.

Validity Test of the Grouting Reinforcement

Both geophysical technology and drilling exploration were performed to test the grouting effects of the 11,050 working face floor. The common approach in geophysical prospecting is the direct current (DC) electric method, which is highly effective in detecting water-rich areas. Drilling is the most direct and accurate method to test the quality of floor grouting reinforcement.

DC Electric Method

The DC electric method is based on the difference in conductivity between the rock layers. By manually supplying a stable current to the ground, the law of the earth current field is observed to determine the characteristics of the geological structure. In the DC detection results, low-resistance anomaly areas mainly indicate areas where the rock formation is broken, a fracture is developed, or the water-abundance is strong. We used the Xi'an Research Institute of China Coal Technology and Engineering Group's model YD32(A). Three DC tests on the 11,050 working face floor were carried out, once before and twice after grouting. The test results are shown in Fig. 8.

From Fig. 8, we can see that three areas experienced low electrical resistivities from the first test data on November 20, i.e., zone A (1640–1740 m from where mining stopped), zone B (1800–1940 m) and zone C (1970–2010 m). The areas of low electrical resistivity in zones A and B were large and located below L_8. It is believed that the L_8 was rich in water in zones A and B; this may be strongly related to water in L_2. The area of zone C was small, and the depth was relatively shallow. It is believed that the hydraulic connection between zone C and L_2 was weak. It also demonstrated that the rock mass of L_8 was initially type III.

Two grouting effectiveness tests were carried out on Nov. 20 and 24, 2015, respectively. The second DC test after grouting was done when the mining working face advanced to 120 m. The results show that the electrical resistivities in zones A, B, and C were highly enhanced, indicating that the grouting had been effective. The state of the rock mass of L_8 was strengthened to type I from type III. However, new areas of low electrical resistivity appeared. Among them, the location of zone D (1710 m) coincided with zone A, but both the width and the depth of zone D were much less than those of zone A. Therefore, the water content in zone D was small but not completely null after reinforcement. The areas of zones E (2100–2160 m) and F (2000–2030 m) were relatively large, but the depths of both zones were relatively shallow,

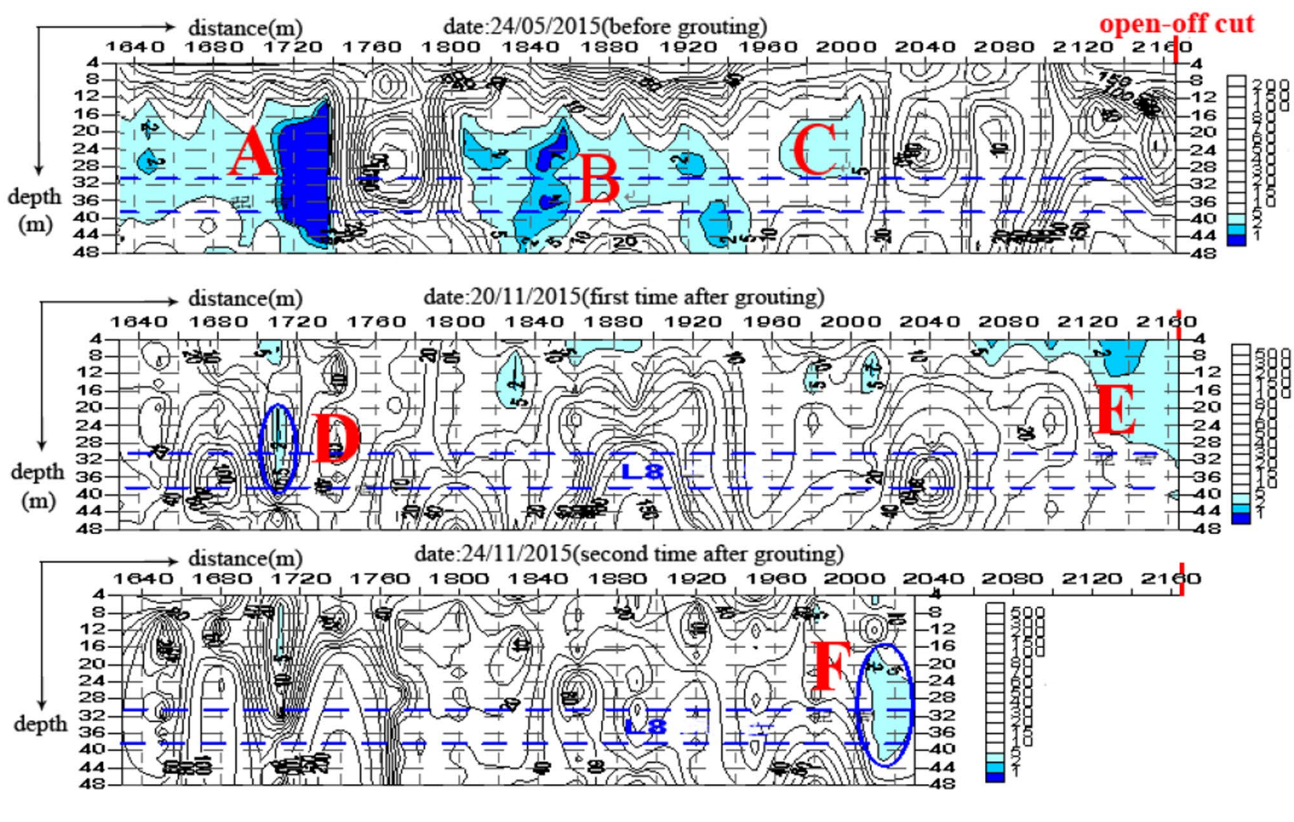

Fig. 8 DC test results along the head-entry of the 11,050 working face

Table 6 Water inflow statistics of the drilling test

Hole no.	Water inflow (m^3/h)	Hole no.	Water inflow (m^3/h)	Hole no.	Water inflow (m^3/h)
D17-10	0.20	D21-9	1.00	U19-8	4.00
D17-11	2.00	D22-11	2.00	U19-9	1.50
D18-11	0.60	D22-12	2.80	U20-7	3.50
D18-12	1.00	U17-5	0.10	U20-8	2.50
D19-12	1.50	U17-7	0.30	U20-10	1.00
D19-13	1.50	U18-6	1.00	U21-11	7.00
D20-10	2.30	U18-8	1.20	U21-12	3.70
D20-3	1.44	U18′-4	1.00	U22-6	3.00
D21-6	6.00	U18′-6	1.40	U22-11	1.60

especially zone E. However, zone E is located at the intersection of the open-off cut and the no. 22 drilling site, where floor deformation was large. Therefore, the analysis suggests that the low electrical resistivity of zone E was caused by infiltration of water from the drilling site. Additionally, the test data showed that zone F was relatively deeper, but that the water content was small. More importantly, this area was close to the working face and did not show a low electrical resistivity during the first test period. It is believed that zone F was caused by water infiltration from the head-entry and fracturing of the rock mass in zone F; mining had changed the state of zone F from type I to type IV.

Drilling Exploration

After all of the grouting projects were finished in the affected areas, at least two test holes were drilled in each drilling site to determine the effectiveness of the grouting reinforcement. As mentioned previously, it was considered safe if the water flow of a single test hole was less than 10 m^3/h. A total of 27 testing holes were drilled in the first 500 m area from the open-off cut. The test results are shown in Table 6.

Table 6 shows that the largest water inflow was 7 m^3/h (D21-11 hole), and the smallest was 0.1 m^3/h (U17-5 hole). Water inflows at all test holes were under 10 m^3/h and clearly reduced compared with those listed in Table 5. Additionally, no floor water inrush occurred during production of the 11,050 working face, which meant that the grouting reinforcement was successful, despite the large mining heights and high water inrush risk.

Summary and Conclusions

There have been too many floor water inrush accidents in the Jiaozuo mining area due to the high hydraulic pressure of floor limestone layers. The 11,050 working face, with a mining height as large as 6.32 m, had a high floor water inrush risk from the L_8, L_2, and Ordovician limestone aquifers. The high mining height leads to a large floor failure depth, and the resulting cracks are more likely to be connected to the aquifer. In order not to reduce the mining height to ensure safe coal mining, the full-floor needs to be grouted and reinforced to fill the cracks and reduce the aquifer water pressure. The floor grouting reinforcement of the 11,050 working face were comprehensively studied, including assessments of the water inrush possibility, the design of grouting technical parameters, and evaluation of grouting effectiveness.

Floor failure depth estimation and water bursting coefficient analysis demonstrated that there was a high water inrush possibility because the estimated depth of the floor failure zone ranged from 21.78 m ~ 37.03 m, which was larger than the average distance between L_8 and the no. 2 coal seam. In addition, the T value of L_8 (0.268) was much higher than the ultimate T_s (0.100).

According to the geological conditions and the preceding analyses, the L_8 limestone, which belongs to a type III jointed rock mass, was the key grouting target. The designed range of the grouting area was 85 m deep below the 2–1 coal seam and 30 m wide outside of the working face borders. The practical grouting pressure was no less than 15 MPa. Clay and cement were the main dry materials of the grouting slurry. To guarantee the grouting quality under a high water pressure, some new grouting methods were used, such as dispersed pulping, transport by thin pipe, and repeated pipe fixation.

Finally, both drilling and DC methods showed that the water inrush probability of the 11,050 working face was significantly reduced, indicating that the grouting reinforcement was successful, despite the large mining heights and high water inrush risk. Most importantly, no floor water inrush occurred during production.

Acknowledgements The authors are grateful to the Zhaogu no. 2 coal mine for their partial funding of the in situ experiments and for providing field-testing sites and related data access. The National Key Basic Research Development Program of China (973 Program 2013CB227903) and the project foundation of Hebei State Key Laboratory of Mine Disaster Prevention (KJZH2017K04) are gratefully acknowledged for their support. Many thanks also for the advice provided by Dr. Yu-bing Gao.

References

Chen LW, Feng X, Xie WQ (2016) Prediction of water-inrush risk areas in process of mining under the unconsolidated and confined aquifer: a case study from the Qidong coal mine in China. Environ Earth Sci 75:706–723

Hu YB, Li W, Liu SL, Liu SL, Wang ZK (2019) Evolution of floor water inrush from a structural fractured zone with confined water. Mine Water Environ 38:252–260

Li H, Bai HB, Wu JJ, Wang CS, Ma ZG, Du YB, Ma K (2017) Mechanism of water inrush driven by grouting and control measures-a case study of Chensilou mine. China Arab J Geosci 10:468

Lu YL, Wang LG (2015) Numerical simulation of mining-induced fracture evolution and water flow in coal seam floor above a confined aquifer. Comput Geotech 67:157–171

Luo LP, Peng SP (2005) Mechanism study on water-inrush hazard of floor strata in mining on confined aquifer. J China Coal Soc 4:459–462 **[in Chinese]**

Meng ZP, Li GQ, Xie XT (2012) A geological assessment method of floor water inrush risk and its application. Eng Geol 143:51–56

Meng L, Feng QY, Li Q (2018) Coupled simulation-optimization model for draining confined aquifer via underground boreholes to prevent water inrush of coal mines. Mine Water Environ 38:93–103

Ren ZC (2015) Construction and practice of water control management system in Baode coal mine. Coal Sci Technol 43(S2):147–150 **[in Chinese]**

State Bureau of Coal Industry (2000) Regulations of coal pillar set and mining of building, water body, railway and main well lane. China Coal Industry Publishing House, Bejing **[in Chinese]**

Sui WH, Liu JY, Hu W, Qi JF, Zhan KY (2015) Experimental investigation on sealing efficiency of chemical grouting in rock fracture with flowing water. Tunn Undergr Space Technol 50:239–249

Wang JA, Park HD (2003) Coal mining above a confined aquifer. Int J Rock Mech Min Sci 40:537–551

Wu Q, Wang M, Wu X (2004) Investigations of groundwater bursting into coal mine seam floors from fault zones. Int J Rock Mech Min Sci 41:557–571

Xu YC, Li JB (2014) "Pore-fractured lifting type" mechanical model for floor water inrush of the grouting enforcement working face. J China U Min Techno 43(01):49–55

Xu YC, Yang Y (2013) Applicability analysis on statistical formula for failure depth of coal seam floor in deep mine. Coal Sci Technol 9:129–132 **[in Chinese]**

Zhang JC (2005) Investigations of water inrushes from aquifers under coal seams. Int J Rock Mech Min Sci 42:350–360

Zhang J, Roegiers JC, Spetzler HA (2004) Influence of stress on permeability around a borehole in fractured porous media. Int J Rock Mech Min Sci 41:454

Zhang GM, Zhang K, Wang LJ, Wu Y (2015) Mechanism of water inrush and quicksand movement induced by a borehole and measures for prevention and remediation. Bull Eng Geol Environ 74:1395–1405

Zhao QB, Zhao XN, Wu Q, Liu CW, Wang XL (2015) Water burst mechanism of "divided period and section burst" at deep coal seam floor in north China. J China Coal Soc 7:1601–1607 **[in Chinese]**

Zhou JR, Yang TH, Zhang PH, Xu T, Wei J (2017) Formation process and mechanism of seepage channels around grout curtain from microseismic monitoring: a case study of Zhangmatun iron mine, China. Eng Geol 226:301–315